Laser and Particle Beams (2003), *21*, 265–272. Printed in the USA.

DOI: 10.1017/S0263034603212155

UV and IR laser radiation's interaction with metal film and teflon surfaces

A.V. FEDENEV, S.B. ALEKSEEV, I.M. GONCHARENKO, N.N. KOVAL', E.I. LIPATOV, V.M. ORLOVSKII, M.A. SHULEPOV, AND V.F. TARASENKO

High Current Electronics Institute, Siberian Branch of the Russian Academy of Sciences, Tomsk, Russia

(RECEIVED 1 April 2003; ACCEPTED 16 May 2003)

Abstract

The interaction of Xe ($\lambda \sim 1.73$ μm) and XeCl (0.308 μm) laser radiation with surfaces of metal and TiN-ceramic coatings on glass and steel substrates has been studied. Correlation between parameters of surface erosion versus laser-specific energy was investigated. Monitoring of laser-induced erosion on smooth polished surfaces was performed using optical microscopy. The correlation has been revealed between characteristic zones of thin coatings damaged by irradiation and energy distribution over the laser beam cross section allowing evaluation of defects and adhesion of coatings. The interaction of pulsed periodical CO_2 ($\lambda \sim 10.6$ μm), and Xe ($\lambda \sim 1.73$ μm) laser radiation with surfaces of teflon (polytetrafluoroethylene—PTFE) has been studied. Monitoring of erosion track on surfaces was performed through optical microscopy. It has been shown that at pulsed periodical CO_2-radiation interaction with teflon the sputtering of polymer with formation of submicron-size particles occurs. Dependencies of particle sizes, form, and sputtering velocity on laser pulse duration and target temperature have been obtained.

Keywords: Adhesion; laser; Teflon; Thin films; Submicron particles

1. INTRODUCTION

From the moment they were engineered, lasers were used both in technologies and in diagnostics. The feature of remote energy transfer and achievement of high energy densities on the target surface allows applying laser radiation as an instrument, for example, in atmospheric probing and surface marking (Rykalin *et al.*, 1985), as well as a source of plasma for spectral diagnostics of material composition (Detalle *et al.*, 2001).

In this work two suggestions for application of pulse laser radiation were investigated. The first suggestion makes use of the fact that the main advantage of laser radiation utilized as a diagnostic test instrument is its remote measurement feature, and at low irradiation energies, data being obtained without damage or slight sample damage. In this article, we suggest using pulsed laser radiation for definition of thin metallic film adhesion to the substrate and film surface defects detection. The preliminary experimental data on Xe and XeCl laser interaction with thin films of metals and TiN-ceramics deposited on glass and steel using technology of vacuum-arc evaporation are presented in the paper by Lipatov *et al.* (2002). Threshold laser radiation power densities necessary for film detachment from the substrate are determined.

The second suggestion relates to IR radiation interaction with polymers. Many polymers have strong absorption bands in the near-IR spectrum region. During polymer surface interaction with laser radiation at a wavelength close to the absorption band, an intensive destruction and removal of target material with a velocity close to the resonance ablation velocity takes place. It should be also taken into account that the absorption band might be shifted during polymer heating by laser radiation. To be a source of laser radiation, most appropriate in the IR region are CO_2 lasers and neodymium lasers possessing high efficiency and a wide range of parameters relating to pulse duration and radiation energy. As for the CO_2 laser, abnormally high absorption was noted for teflon (Tolstopyatov *et al.*, 1998). The interaction of pulsed repetitive CO_2 ($\lambda \sim 10.6$ μm) and Xe ($\lambda \sim 1.73$ μm) laser radiation with teflon surfaces has also been studied in this article.

Address correspondence and reprint requests to: Andrei V. Fedenev, High Current Electronics Institute SD RAS, 4 Akademichesky Ave., 634055 Tomsk, Russia. E-mail: fedenev@loi.hcei.tsc.ru

2. EXPERIMENTAL EQUIPMENT AND TECHNIQUES

In our experiments we used three laser setups. The general parameters of the setups employed in experiments are listed in Table 1. Setup 1 was based on the e-beam preionized discharge laser (Tarasenko *et al.*, 1998, Orlovskii *et al.*, 1998). The parallel-plane resonator provided laser radiation divergence of about 1.6 mrad. Water cooling systems of the output foil window and operating mixture circulation at flow velocity of about 10 m/s allowed operation at pulse repetition rate (p.r.r.) of up to 25 Hz. During use of the mixture Ar:Xe = 100:1 at a pressure of 1 atm, the main part of the laser energy was radiated at $\lambda = 1.73$ μm and the laser provided an impulse energy of 10–15 mJ at a duration of about 320 ns. With a CO_2 laser gas mixture, this setup provides a laser pulse at $\lambda = 10.6$ μm with energy of 3–10 J and a pulse duration of 100 ns–20 μs, depending on gas mixture composition.

Setup 2 was presented by a wide-aperture laser (output window diameter was 20 cm) pumped by a radially convergent electron beam (Tarasenko *et al.*, 1998). With a mixture ratio of Ar:Xe = 100:1, $p = 2.5$ atm, (the basic wavelength of lasing was 1.7 μm), and a parallel-plane resonator formed by an aluminum-covered mirror and a quartz plate, the lasing energy at the target surface focused by an optics system consisting of three quartz lenses to a spot 5 mm in diameter was at 5 J with a laser pulse duration of 400 ns.

For setup 3, the FOTON-class electro-discharge laser (Verkhovskii *et al.*, 1995) with an output energy of 19 mJ ($\lambda = 308$ nm) and 8 mJ ($\lambda = 222$ nm) was taken. The lasing wavelength varied with a change of gas mixtures. An unstable telescopic resonator with index of ~6.7 was used in experiments. The lasing pulse durations at FWHM were 20 ns and 12 ns for $\lambda = 308$ nm and $\lambda = 222$ nm, respectively.

Laser energy and average power were measured by a calorimeter IMO-2N and pyroelectric sensor PE-25 (OPHIR Opt.) calibrated in the measuring optical range with inaccuracy of 5%. For investigation of irradiated surface properties, optical microscopes of the MMR-4 type (LOMO, ×1500 maximal magnification) and microinterferometer MII-4 (LOMO) were used.

3. RESULTS AND DISCUSSION

3.1. Deformation, destruction, and detachment of thin metallic film from glass surfaces by laser radiation interaction

The stainless steel and niobium films deposited using the vacuum-arc method (Schanin *et al.*, 2000) were irradiated. To increase adhesion of coating to the substrate, the surface of the glass was initially cleaned in a plasma of Ar glow discharge ($p \sim 10^{-3}$ mm Hg, $I = 60$ A). The film thickness was about 300–1000 nm.

The 1-μm niobium layer deposited on glass was irradiated using the pulsed Xe laser (setup 1; the thickness of the glass substrate was 5 mm). The radiation power density on the target surface varied with the changing distance from the lens (BaF_2, $F = 123$ mm). The focus spot diameter was of the order of 300 μm. Maximum radiation energy density in the focal spot was about 20 J/cm^2. The experiments were conducted in air at a perpendicular laser beam incidence on the surface irradiated. Dependence of the damaged area on the distance from the lens for the cases of direct and "indirect" (through the glass) interaction are demonstrated in Figure 1. With laser radiation passing through the glass, the spot diameter increases at the output, with about 30% of the energy absorbed by the glass substrate; nevertheless, in the case of indirect focusing, the size of the damaged area of the Nb thin film at the same distance from the lens is greater than at direct focusing. The two characteristic inflection points on the plots should be mentioned. Before the first

Table 1. *Parameters of laser setups used in experiments*

Setups	Pumping technique, Active medium, P.r.r.	Transitions, Wavelengths, Gas mixture, pressure	Pulse duration, Energy, Efficiency
"CASCADE"	E-beam initiated discharge, $72 \times 3 \times 2.4$ cm^3, p.r.r.: 25 Hz	Xe, 1.73 μm, Ar-Xe CO_2, 10.6 μm, CO_2-N_2	300 ns, 15 mJ, 100 ns–20 μs, 3–10 J
"ELON-1M"	Electron beam, $j = 40$ A/cm^2, 31 L, aperture D = 20 cm, single pulse regime	Xe, 1.73 μm, 2.03 μm, Ar-Xe, He-Ar-Xe	400 ns, 20 J, ~2%
"PHOTON-2"	Discharge, $2.5 \times 0.5 \times 60$ cm^3, 1 Hz	XeCl, 308 nm, HCl-Xe-Ne KrCl, 222 nm, HCl-Kr-Ne	20 ns, 120 mJ 12 ns, 70 mJ

https://doi.org/10.1017/S0263034603212155 Published online by Cambridge University Press

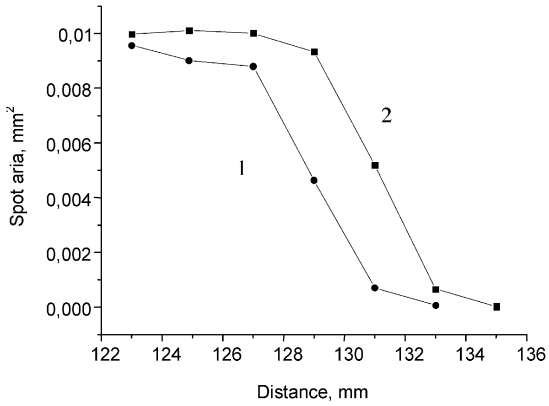

Fig. 1. Dependence of damaged area diameter from distance to focusing lens for direct (1) and indirect (through glass substrate) (2) irradiation of Nb-film (0.3 μm thick) by Xe laser (setup 1).

inflection point (at distances close to the focal one) mainly coating evaporation and cracking of the glass substrate surface occurs. In the second area (between the first and second inflections), the main process is metal melting. And in the area maximally distant from the focus areas with still visible surface damages, the absorbed energy is sufficient only for cracking and "flaking off" of the coating. The processes of coating evaporation and melting have threshold character by temperature determining presence of inflection points on the curves.

The same sample was used in experiments with Xe laser radiation (setup 2), at an energy density on the target surface of about 20 J/cm^2 and a spot diameter in the focal area of about 5 mm. Figure 2 is a micrograph of part of the laser imprint on Nb film as well as separate characteristic zones of the spot with great magnification. In the central zone, the

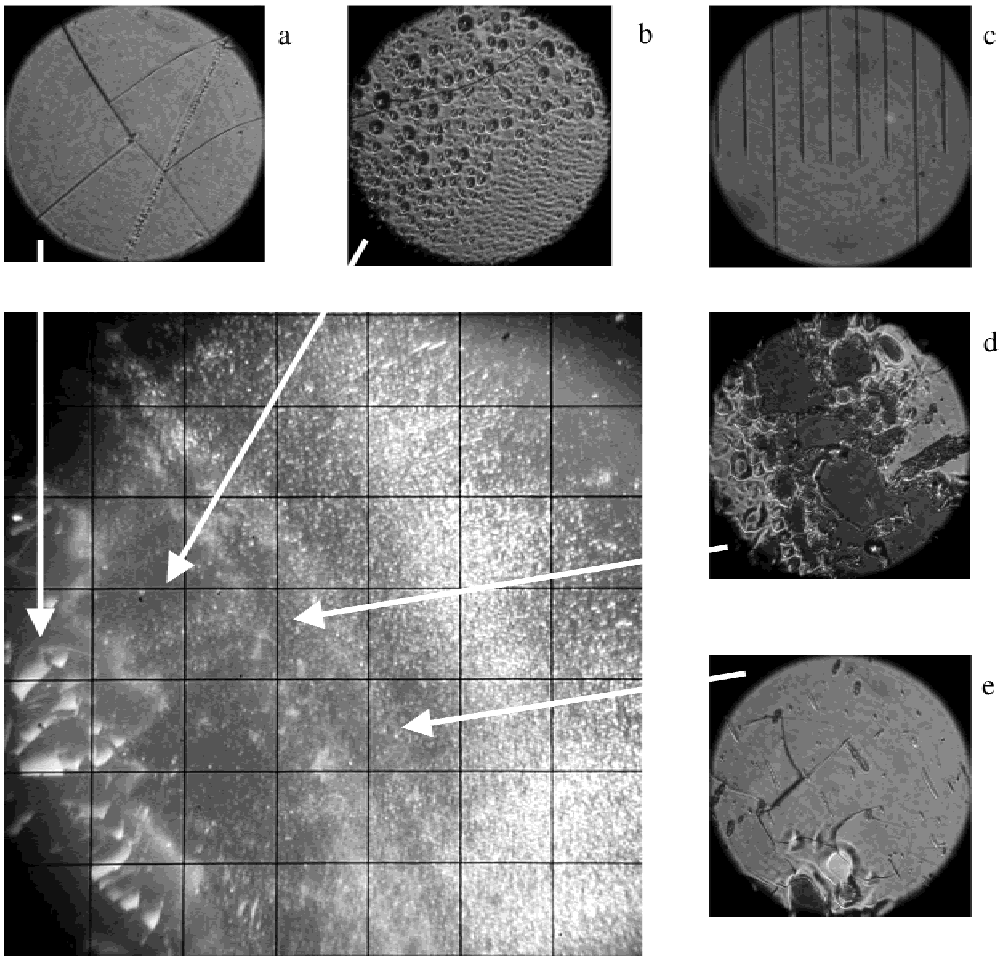

Fig. 2. Micrographs of Nb thin film surface deposited on a glass substrate after irradiation by Xe laser (setup 2). Damaged zones of film: (a) cracking of glass substrate surface; (b) droplets of metal are fused into glass and cracking of glass surface takes place; (d) melting of metal film; (e) metal film is cracking and flaking off. (c) scale (10 μm between strokes). Length of square side in main photo is 1/7 mm.

https://doi.org/10.1017/S0263034603212155 Published online by Cambridge University Press

metallic film is totally evaporated and the glass surface is covered with fine cracks and peeled flakes. Moving away from the center, it is possible to distinguish three other main zones differing in size and the character of the surface damage. In zone 1 (Fig. 2b), the surface of glass substrate has also been cracked and covered with metallic microscopic size droplets fused into glass. Separated parts of the metallic film with uneven molten edges are characteristic for zone 3 (Fig. 2d); the surface of the glass is not damaged. In the fourth zone (Fig. 2e), the metallic film has been cracked and metal flakes have been separated from the substrate. In the periphery of the laser irradiation zone, the surface of the Nb film is covered with sputters of metal and oxides ejected from the interaction zone. The joint width of zones 2, 3, and 4 is approximately 20% of the spot radius. Similar characteristic damage zones were monitored as well at irradiation of the stainless steel film on glass substrate. It differed from the Nb film in the existence of some surface areas in the central zone covered with "freezing patterns" of crystals fused in glass. To determine the origin of such crystals, it is necessary to perform additional experiments.

The same samples were irradiated by a nanosecond UV laser (setup 3) with uniform in aperture energy distribution. Through energy density variation in the target plane, the characteristics of damage in zones No. 2–4 was obtained. Figure 3 presents micrographs of XeCl laser imprints on 1-μm stainless steel film deposited on a glass substrate. With surface power density $W \sim 21$ MW/cm^2, the film changes color but slightly. An increase in lasing power up to $W \sim 50$ MW/cm^2 results in thin film cracking and flaking off over practically the whole interaction area (see Fig. 3a). A further power density increase up to 82 MW/cm^2 results in droplet formation on the film surface (Fig. 3b). Neither film detachment nor cracking are observed in this case, which implies that due to heating by laser radiation, the surface temperature has exceeded the threshold of plastic deformation. Further, at $W \sim 144$ MW/cm^2, the metallic coating was melted over the total surface of the interaction (Fig. 3c). The maximal laser power density of 474 MW/cm^2 used in our experiments led to total evaporation of the metal thin film over the spot irradiated and surface cracking of the glass substrate (Fig. 3d).

Energy density threshold values of the laser radiation necessary for peeling of a number of coatings (Ti, Zr, TiN, Cu, Nb) and substrates were defined. For example, the value of the threshold density at $\lambda \sim 308$ nm necessary for zirconium film detachment from glass (thickness is 0.3 μm) is of the order of 35 MW/cm^2.

3.2. Laser radiation interaction with TiN-ceramics

The Xe laser with the same output parameters (setup 1) was used for irradiation of 1-μm TiN film deposited by the vacuum arc technique on the surface of 4140-type steel (Schanin *et al*., 2000). Microscopic study had shown that after single-pulse irradiation the surface in the central zone had changed color to gray-metallic, which means nitrogen extraction from the surface layer, and melted. Near the outside spot edge, at the crater boundary there is a narrow zone where the coating has been cracked and broken away from the substrate. The round-up of the blue and brown color around the spot is most probably connected with oxidation of the Ti evaporated from the central region. Rather different results were obtained after irradiation of the same TiN film by a UV laser with a 20-ns pulse duration. At a specific radiation energy of about 9 J/cm^2, the film surface had also changed color to light gray, but instead of melting, it was cracked with micron-width cracks (see Fig. 4b). In this case, colored surroundings were absent. Melting of the film surface and, after about 20 pulses, the complete TiN film evaporation occurred with increasing of the pulse number.

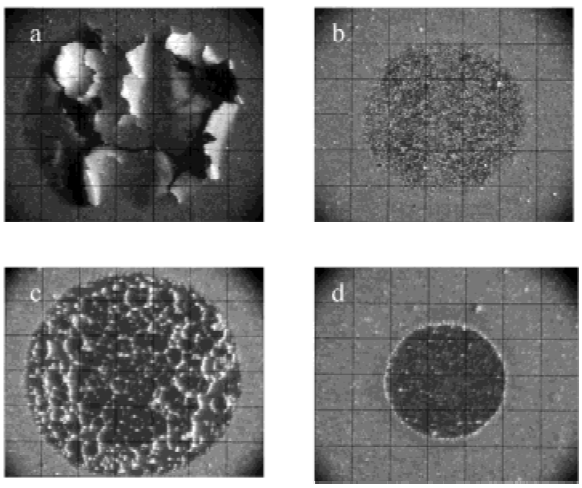

Fig. 3. Micrographs of stainless steel film surface, deposited on glass substrate and modified by pulsed XeCl laser radiation. a: power density $W = 50$ MW/cm^2. b: $W = 82$ MW/cm^2. c: $W = 144$ MW/cm^2. d: $W = 474$ MW/cm^2. Lengths of square side are 1/4 mm (a,b,c) and 1/7 mm (d).

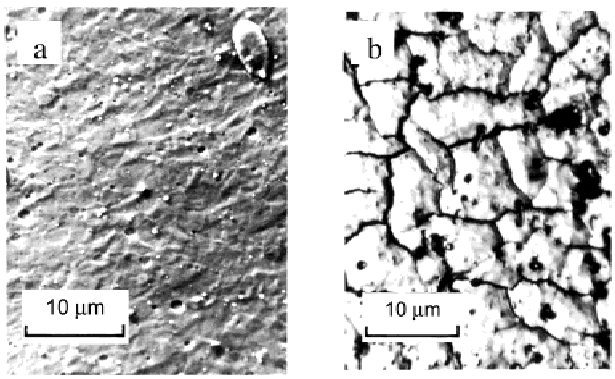

Fig. 4. TiN thin film surface: (a) original, SEM image; (b) after irradiation by XeCl laser ($\tau = 20$ ns, specific energy 9 J/cm^2), optical microscope image.

https://doi.org/10.1017/S0263034603212155 Published online by Cambridge University Press

3.3. Teflon (PTFE) sputtering by 10-μm laser radiation

In our experiments, PTFE plates 2.0 and 7.5 mm thick and with a density of $2.2 \cdot 10^{-3}$ g/mm^3 produced at Kirovo-Chepetsk chemical plant were used. Radiation of the CO_2 laser was focused on the teflon surface using an NaCl lens. The plate could be heated up to ~150°C by an air heating gun with power and air temperature slide control being installed from the its reverse side. Teflon face side temperature was controlled through a thermocouple placed ~3 mm from the laser radiation interaction point.

A crater with even edges without traces of melt or blackening was formed after irradiation of the teflon plate surface by focused pulsed radiation of the CO_2 laser with p.r.r. of ~1 Hz. The crater sizes were determined not only by the number of laser pulses and pulse energy density but also by the pulse duration and the initial temperature of the target surface. In the experiments, the teflon plate was irradiated by CO_2 laser pulses of various durations until a through hole appeared. Experimental results of teflon irradiation at a surface temperature of 20°C are listed in Table 2.

The hole sizes and the mass of dispersed teflon at irradiation by both types of pulses are comparable. In the case of short pulse irradiation (type A), 120 laser shots were required to obtain a through hole, whereas for irradiation by type B, 30 pulses were needed for the hole to appear. At irradiation by long pulses (type B), the specific mass of teflon removed from the interaction zone per pulse is almost six times greater than that for A-type pulse treatment. The laser power density on the surface for the short pulse treatment is two orders greater than that for B-type pulses; however, the energies of the pulses were comparable. It should be noted that a part of the laser energy was absorbed by plasma of spark occurred in air during radiation by type A pulses focussed on surface of polymer.

For the both pulse types, increasing of the PTFE surface temperature resulted in an increase of the efficiency of teflon mass removal from the crater (Fig. 5). At a surface temperature of 130°C on average $15.2 \cdot 10^{-4}$ g of teflon material is removed from the crater per 15-μs pulse (type B). The increase of mass removal velocity versus temperature rise is faster wth treatment by long pulses (type B).

For determination of the type and sizes of the particles removed from the crater during laser irradiation, a quartz plate was placed vertically at a distance of ~6–8 mm from the treatment zone. After nearly 30 shots of the CO_2 laser, a whitish spot was formed on the quartz surface, and the spot transparency increased with distance from the radiation zone. At short pulse laser interaction, the particles were removed out of the crater for longer distances. Figure 6 shows photomicrographs of the quartz plate regions at distances of 5 and 15 mm from the target at laser pulse duration of 15 μs. The surface is covered with irregularly shaped particles of sizes from 0.5 μm up to several tens of microns. The sizes and form of particles differ depending on the distance from the target. The number of big particles is mostly high at close distances. The big particles have a grain structure with grain sizes of 0.5–1 μm. Fiberlike formations are observed on the quartz surface at a distance of ~15–20 mm from the target. The thickness of the fibers is ~0.5–1 μm; the length is from 5 to 50 μm (see Fig. 6b). The particles of submicron sizes are mainly observed at distances of 40 to 50 mm from the target surface. In the case of high density of particles deposited on the quartz surface in the near-target region, the small particles stick together forming bigger particles.

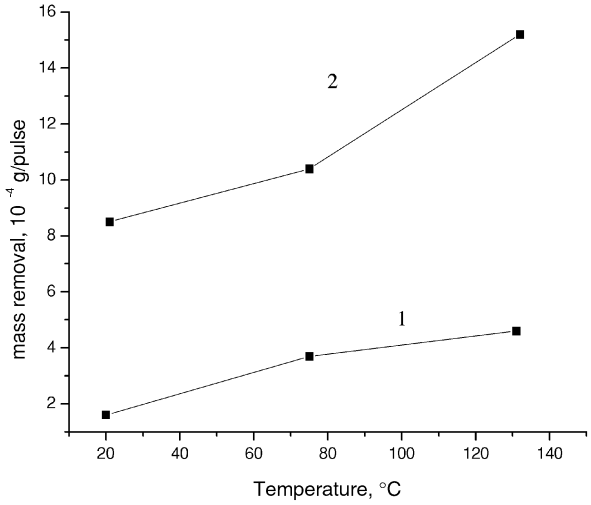

Fig. 5. Dependence of the teflon mass removal per pulse versus surface temperature of PTFE plate. 1: A-type pulse. 2: B-type pulse.

Table 2. *Basic conditions and results of experiments on quantification of average teflon being removed from crater per pulse of CO_2 laser radiation (T ~ 20°C)*

Pulse type	Pulse energy, J	Power density, W/cm^2	Number of pulses	Dispersed mass, g	Mass removal per pulse, g/imp
A (100 ns)	4.2	$4.12 \cdot 10^8$	120	$19.1 \cdot 10^{-3}$	$1.47 \cdot 10^{-4}$
B(15 μs)	5.6	$3.2 \cdot 10^6$	30	$25.6 \cdot 10^{-3}$	$8.5 \cdot 10^{-4}$

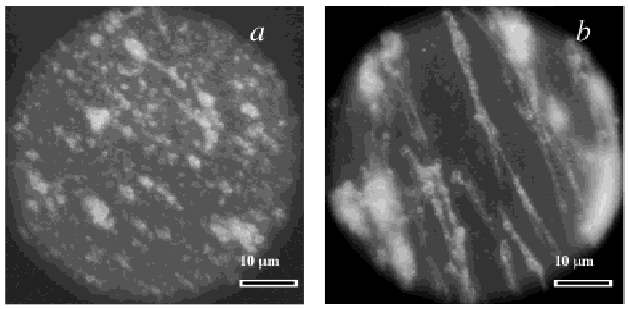

Fig. 6. Micrographs of quartz plate surface with teflon particles deposited during 30 pulses (type B, 15 μs) by a CO_2 laser: (a) distance from target is 5 mm, (b) distance from target is 15 mm. Surface temperature is 21°C.

https://doi.org/10.1017/S0263034603212155 Published online by Cambridge University Press

The micrographs were scanned and numerically processed to define the size distribution of powder. The surface processed was 87×67 μm^2. Figure 7 presents the dependencies of particle number distribution versus their size in the quartz plate region 45 mm from the target. In the experiments, the teflon surface temperature was 80°C and 134°C in Figure 7a and Fig. 7b, respectively. It should be noted that the minimal size of the particles registered using the above mentioned method is limited by microscope resolution and image numerical processing. According to our estimations, the minimal size of particles is of the order of 0.3 μm. At short pulse irradiation (type A), the majority of teflon sputtered particles are 1–2 μm in size (Fig. 7a), whereas at long pulse irradiation of 15 μs the number of particles with sizes >2 μm becomes greater. For both irradiation modes, increasing the temperature of the target surface results in growth of the number of bigger particles (see Fig. 7b).

Different results were obtained wth teflon irradiation by an Xe laser (setup 2, $\lambda = 1.73$ μm). At specific energy of ~ 20 J/cm^2 on target surface, the teflon was slightly melted accompanied by foliation and the appearance of small black spots. After one shot of the Xe laser, the 50-μm film was broken through over the contour of the laser radiation spot; teflon sputtering was not observed.

3.4. Discussion

In general, pulsed laser radiation interaction with matter may be characterized by the following processes, namely, photon energy absorption by the surface; transformation of energy in radiative and nonradiative processes; fast heating and cooling of the target; ablation, melting, evaporation, and ejection of target matter out of the interaction zone; and ionization and formation of plasma. At low densities of laser radiation energy, the heating and oxidation of metallic film (change in color) occur. With increasing of the energy density, the temperature of the metallic film increases faster than the temperature of the glass substrate (in our experiments: glass thermal conductivity is ~ 1 W/m·degree K, and for niobium it is 56 W/m·degree K; their coefficients of linear thermal expansion are comparable). The mechanical stresses occur as a result of thermal expansion of the metal at the metal–glass boundary. The film detachment occurs in the case when the value of mechanical stress exceeds the value of film adhesion. As the power density of the laser radiation and temperature of the film are increasing, the film is heated up to the temperature of plastic deformation and further melting. In this case, the film detachment from the substrate does not occur and film deformation looks like the surface is covered by droplets and fused "islands" of melted metal. With a further increase in energy density, the film evaporates and if the melting temperature of the substrate is lower than that of the coating, the fusion of the film material droplets into the substrate occurs. In our experiments, the glass surface was cracked due to mechanical stresses connected with the thermal gradient. The processes of melting and evaporation are initiated at definite temperatures of phase change and this is probably the reason for the presence of characteristic inflection points on the plot of the dependence of the damaged area on radiation power density (see Fig. 1).

At irradiation from the reverse side (through the glass substrate), besides the thermal deformations tearing the film off the substrate, the vapor pressure of the melted thin film material (or probably the upper melted layer of glass substrate) acts in the same way. As a result, the efficiency of film detachment by irradiation through the glass substrate is higher than in the case of direct irradiation despite the essential absorption inside the glass.

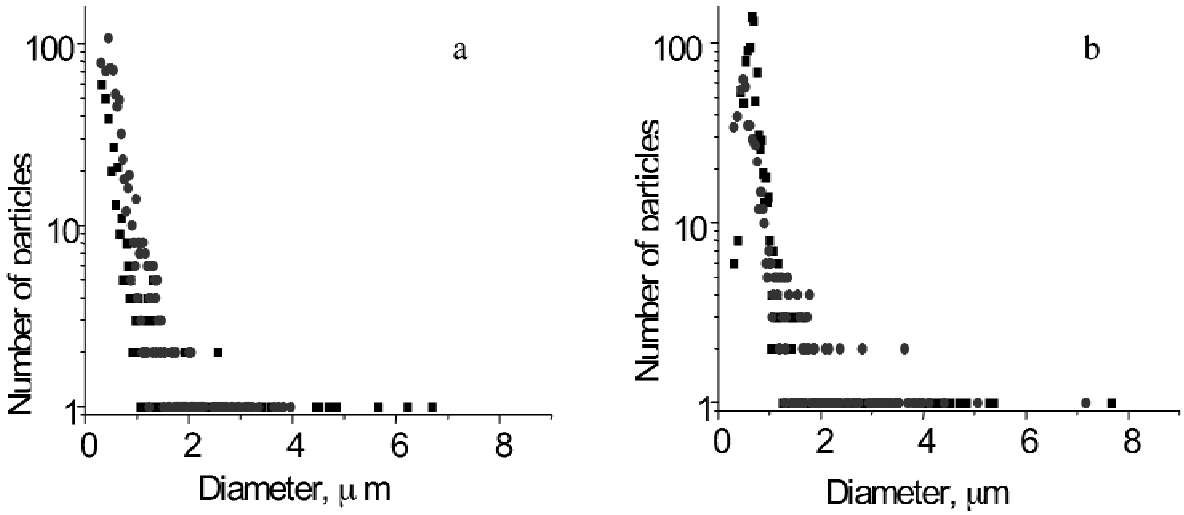

Fig. 7. Number of particles deposited on quartz plate versus their size. Distance from target surface is 45 mm. Temperature of teflon is 80°C (a) and 134°C (b). CO_2 laser pulse duration is: 100 ns (■), 15 μs (●).

https://doi.org/10.1017/S0263034603212155 Published online by Cambridge University Press

Actually, if in the central zone the radiation energy is sufficient for metal film evaporation, in zone 2, the temperature is enough only for metal boiling accompanied by further formation of droplets. In zone 3, the energy is still sufficient for fusion (mostly efficient on coating defects). Eventually, in zone 4, the absorbed energy of the laser radiation is not enough for metal melting, but the difference in thermal conductivity of materials used for the coating and substrate leads to the initiation of mechanical stresses in the region of the coating–substrate boundary and detachment of the coating. The coating adhesion is characterized by the energy necessary to remove the coating from the substrate, that is, as a first approximation, the energy is equal to the value of the mechanical stress sufficient for detachment of the coating from the substrate. The laser with predetermined (e.g., Gauss) beam energy density distribution over a cross section may be used in express diagnostics of thin film coating adhesion through measuring the coating damage diameter after irradiation.

In irradiation of TiN film on a steel substrate we have different pictures of deformations. At similar laser radiation parameters, the width of the boundary zone of coating cracking is much narrow than in the case of our experiment with metallic coatings deposited on a glass substrate. That is determined by less difference in the thermal conductivity of the coating and the substrate (steel) and the comparable value of the modulus of elasticity for TiN and steel. The experiments on the interaction of a 20-ns XeCl laser with TiN film deposited on the stainless steel substrate have shown that the coating adhesion in this case is close to or exceeds the values of mechanical stresses resulting from the laser heating. The surface of TiN film is cracking and slightly melting (see Fig. 4b), but does not separate from the substrate.

Yakovlev (1981) used laser radiation to determine adhesion of thin absorbing films. The following mechanism of coating deterioration was supposed (see either Veiko *et al*., 1980*a* or 1980*b*). Under the influence of pulsed laser radiation (about 1 μs in duration), the total melting-through of the film occurs in the center of the spot and the partial melting and evaporation of the upper layer of metallic film is present over the whole surface subjected to interaction. The melt starts to move due to surface tension forces of liquid metal and vapors pressure and the edges of the film detach and become twisted, starting with the center of the laser radiation spot. In modeling such processes, a system of equations is solved for thin film thermal conductivity on substrate made from other material taking into account averaged by area contact (adhesion) and motion equation of the melted metal taking into account surface tension forces. Qualitative dependencies of adhesion influence on thin metallic films under laser radiation were presented.

Zhou *et al*. (2002) reported that laser-driven shocks (at a pulse duration of about 1 ns or less) could lead to a dynamic failure, called film spallation. They used a modified laser spallation setup to measure the dynamic adhesion of thin films and proposed a novel diagnostic technology. Based on correlation theory, new spallation criteria for characterizing the progressive damage at the interface between the film and the substrate were established, such as interface delamination, film spallation, and film expulsion. With the help of the theory, the degree of damage and the dimension of damage (i.e., fracture), such as the minimum width of delamination radius, the thickness of the film, and so forth, were estimated. Experiments were carried out on epoxy/stainless steel and epoxy/Al, and the experimental results show that their dynamic bonding strengths are about 25 MPa and 20 MPa, respectively.

In contrast to the laser radiation conditions [high energies, high power, and short pulse duration (1 ns or less)] used in the above mentioned papers, we suggest using irradiation of thin films by a UV laser with a duration of $\sim$20 ns and energy density on the target of about 0.5–1 J/cm^2, which is not sufficient for film melting and evaporation but provides significant thermal stress built up in the film to separate it from the substrate. Thus, the cost of laser setup and cost of the device for adhesion measurements will be essentially decreased.

The preliminary theory explaining anomalous high velocities of teflon destruction under irradiation by CW CO_2 laser is presented in the paper by Tolstopyatov *et al*. (1998). As polymer temperature increases, absorption rises due to the broadening of absorption bands of vibrational modes of macromolecules. Because PTFE is a high crystalline polymer, it has an ordered structure even at temperatures exceeding its melting temperature (600°K). Complete decomposition of supermolecular structure occurs if the heating time is over 15 min at 723°K. It is difficult to assume that different phases of polymer could absorb laser radiation differently. Local heating may proceed owing to the presence of other absorption centers (impurities). As the temperature reaches $\sim$700°K, macromolecules start degrading with the formation of monomers of tetrafluoroethylene (TFE). The monomer absorption band lies near the wavelength of the CO_2 laser even at room temperature. The small TFE bubbles formed in the polymer bulk act as active absorption centers for the energy of the laser radiation, enhancing the rate of polymer decomposition.

In our experiments, with different laser pulse duration, mass removal per shot was different probably due to the occurrence of spark in the air above target surface during A-type pulse treatment when a part of the energy was absorbed by the plasma. At relatively long laser pulses and a power density of $\sim 10^6$ W/cm^2 the bubbles of monomer act as the main absorbers of laser radiation energy. Being heated, they are replenished with new TFE molecules due to thermal decomposition of nearby polymer, and pressure inside the bubbles increases. The viscosity of the polymer around the bubble decreases with the temperature rise, allowing the bubble to increase its volume. It results in the polymer breaking off into rather big particles. The amount of teflon sputtered per shot is relatively big; at repetitive pulsed irradiation the crater rapidly increases in size, and the size of particles

https://doi.org/10.1017/S0263034603212155 Published online by Cambridge University Press

is over 10 μm. At short pulse irradiation (~100 ns) and power $W \sim 10^8$ W/cm^2, monomer bubbles are heated and an increase of pressure inside them occurs during less time, and the viscosity of the polymer around the bubbles has no time to change. The bubbles are smaller in size than in the case of slow heating of the polymer. This results in higher pressure inside the bubbles, and in their breaking off, the particles acquire greater initial velocities and leave the crater for greater distances. External heating of the target leads to growth of absorbing center density and a decrease in polymer viscosity, resulting in faster decomposition of PTFE and a greater number of big particles and fiberlike filaments removed from the crater under irradiation.

4. CONCLUSION

The possibility of thin film adhesion testing by focused pulsed laser irradiation with known power distribution over cross sections has been demonstrated. The adhesion value can be estimated through measurements of the damaged area size. This method is very promising in testing of adhesion of films with relatively different substrate temperature conductivity and thermal conductivity, for example, those deposited on glass metallic and metal-ceramic films. The use of this method is limited by the case where the adhesion value is high and the difference in the thermal conductivity of the substrate and the film material is low. This is the situation when the temperature stress is not sufficient for film detachment, but the surface heating temperature provided by laser radiation is enough for initiation of plastic deformations and film melting.

The correlation between the parameters of surface erosion (the area of the crater and the amount of evaporated material versus the laser focus position and the number of pulses) was investigated during the interaction of CO_2 laser radiation on the PTFE surface. Monitoring of the erosion track on surfaces was performed through optical microscopy. It has been shown that at pulsed periodical CO_2 radiation interaction with teflon the sputtering of the polymer with the formation of submicron-size particles occurs. Dependencies of particle sizes, form, and sputtering velocity on laser pulse duration and target temperature have been obtained. The process of anomalous teflon decomposition close to resonance ablation under irradiation by a CO_2 laser can be used for production of teflon powder consisting of particles of sizes of the order of a micrometer. Increasing of the teflon target surface temperature or laser pulse duration results in a greater amount of PTFE mass being sputtered per shot, an increase in particle sizes, and the appearance of fiberlike formations. Teflon sputtering velocities and powder particle distribution by size at a pulse duration of 100 ns and 15 μs and specific powers of 10^8 and 10^6 W/cm^2, respectively, have been defined.

REFERENCES

Detalle, V., Sabsabi, M., Heon, R. & St-Onge, L. (2001). Improvement of depth profile analysis by laser induced plasma spectroscopy. *Proc. of COLA-01*, p. 177, Tsukuba, Japan.

Lipatov, E.I., Fedenev, A.V., Alekseev, S.B., Goncharenko, I.M., Koval', N.N., Orlovskii, V.M., Tarasenko, V.F. & Shulepov, M.A. (2002). Study on interaction of Xe and XeCl-laser radiation with metal films. *Proc. of 6th Int. Conf. on Modification of Materials with Particle Beams and Plasma Flows*, pp. 484–487. (Mesyats, G.A., Korovin, S.D. & Ryabchikov, A.I., Eds.). Tomsk, Russia: Kursiv.

Orlovskii, V.M., Poteryaev, A.G. & Tarasenko, V.F. (1998). CO_2 lasers pumped by e-beam controlled discharge and e-beam ignited discharge. *Proc. of LASERS'97*, New Orleans, LA. pp. 754–760. (Carroll, J.J. & Goldman, T.A., Eds.). McLean, VA: STS Press.

Rykalin, N.N., Uglov, A.A., Zuev, I.V. & Kokora, A.N. (1985). *Laser and E-Beam Treatment of Materials (Handbook)*. Moscow: Mashinostroenie.

Schanin, P.M., Koval, N.N., Goncharenko, I.M., Grigorjev, S.V. & Tolkachev, V.S. (2000). Interaction of the droplet fraction of a vacuum arc with the plasma of a gas discharge. *J. Tech. Phys.* 177–184.

Tarasenko, V.F., Baksht, E.H., Fedenev, A.V., Orlovskii, V.M., Panchenko, A.N., Skakun, V.S. & Sosnin, E.A. (1998). Ultraviolet and infrared lasers with high efficiency. *SPIE Proc. of the Int. Conf. on High Power Laser Ablation*. Vol. 3343, pp. 715–724.

Tolstopyatov, E.M., Ivanov, L.F., Grakovich, P.N. & Krasovsky, A.M. (1998). Destruction of polytetrafluorethylene under the action of carbon dioxide laser radiation at low pressure. *SPIE Proc. of the Conf. on High Power Laser Ablation*. Vol. 3343, pp. 1010–1017.

Veiko, V.P., Metev, S.M., Kaidanov, A.I., Libenson, M.N. & Jakovlev, E.B. (1980*a*). Two-phase mechanism of laser-induced removal of thin absorbing films: I. Theory. *J. Phys. D: Appl. Phys.* **13**, 1565–1570.

Veiko, V.P., Metev, S.M., Stamenov, K.V., Kalev, H.A., Jurkevich, B.M. & Karpman, I.M. (1980*b*). Two-phase mechanism of laser-induced removal of thin absorbing films: II. Experiment. *J. Phys. D: Appl. Phys.* **13**, 1571–1575.

Verkhovskii, V.S., Lomaev, M.I., Panchenko, A.N. & Tarasenko, V.F. (1995). 'Foton' series of universal pulsed lasers. *Quantum Electronics* **25**, 5–7.

Yakovlev, E.B. (1981). Influence of adhesion on laser heating and damage of thin absorbing films. *Sov. Quantum Electronics* **8**, 1073–1078.

Zhou, M., Zhang, Y.K. & Cai, L. (2002). Adhesion measurement of thin films by a modified laser spallation technique: Theoretical analysis and experimental investigation. *Appl. Phys. A: Materials Science & Processing* **74**, 475–480.

https://doi.org/10.1017/S0263034603212155 Published online by Cambridge University Press